Journal of Naval Architecture and Marine Engineering
December, 2024
http://dx.doi.org/10.3329/jname.v21i2.70221 *http://www.banglajol.info*

HEAT TRANSFER INTENSIFICATION IN A HORIZONTAL TUBE UTILIZING HEXAGONAL PERFORATED TUBE INSERTS

Md. Zohurul Islam[1], Goutam Saha[2*], Yong Sheau Chin[3] and Suvash C. Saha[3]
[1]Department of Mathematics, Jashore University of Science and Technology, Jashore 7408, Bangladesh
[2*]Department of Mathematics, University of Dhaka, Dhaka 1000, Bangladesh, Email: ranamath06@gmail.com
[3]School of Mechanical and Mechatronic Engineering, University of Technology Sydney, Ultimo, NSW 2007, Australia

Abstract:

In response to the century-long demand for heat energy, efficient use, conservation, and recovery of heat have become critical issues. Heat exchanger manufacturing, with its substantial capital and operational costs, now necessitates an efficient and energy-saving approach. Various methods have been developed over the years to enhance heat transfer within these systems to improve performance and reduce fuel consumption. One such approach is passive heat transfer enhancement, which involves introducing geometric alterations in the flow medium, such as using inserts or modifying the tube surface. This study aims to examine flow and heat transfer behavior within a horizontal tube, employing hexagonal perforated tube (HPT) inserts with varying diameter ratios (DR). To achieve this, a 3D model of the HPT inserts was developed and analyzed using finite volume based ANSYS Fluent software. The investigation considered Reynolds numbers (Re) within laminar flow regions, ranging from 1118 to 1676 while exploring HPT inserts with DR of 0.167, 0.238, 0.357, and 0.476, respectively. Results reveal that the Nusselt number (Nu) is notably influenced by both Re and DR of the HPT inserts. The enhancement in Nu achieved through the use of HPT inserts can reach up to an impressive 60.4% compared to the plain pipe's performance, offering substantial benefits in terms of energy conservation and system performance.

Keywords: Heat Transfer; Horizontal pipe; Hexagonal perforated tube; Diameter ratios; Reynolds number;

NOMENCLATURE

C_p	Specific heat ($Jmol^{-1}K^{-1}$)	p	Pressure (Nm^{-2})
D	Diameter (m)	Re	Reynolds number
DR	Diameter ratios	T	Temperature (^oC)
HE	Heat exchanger	TT	Twisted tapes
HT	Heat transfer	$\vec{v}$	Velocity vector (ms^{-1})
HPT	Hexagonal perforated tube	***Greek Symbols***	
Nu	Nusselt number	ρ	Density (kgm^{-3})
PTT	Perforated twisted tapes	μ	Dynamic viscosity ($Pa\ s$)
		κ	Thermal conductivity ($Wm^{-1}K^{-1}$)

1. Introduction

The growing interest and demand for heat exchangers (HE), as indicated by market projections of surpassing $13 billion by 2025 (HEMT, 2019), have prompted numerous researchers to explore cost-effective alternatives for enhancing heat exchanger efficiency. Improving HE efficiency translates directly to enhanced heat transfer (HT) rates with minimal energy and material expenses. In the realm of passive HT enhancement techniques, which involve the incorporation of inserts into heat exchanger tubes, various insert types have been employed and investigated to boost HT rates (Dhumal et al., 2017; Bhattacharyya et al., 2022; Ali et al., 2023). Among these, brush inserts, coil wire inserts, twisted tape inserts, and mesh inserts are commonly used (Paneliya et al., 2020; Mohammad et al., 2013; Kundan and Darshan, 2022). Indeed, the practice of augmenting mixed convection HT by employing inserts in cylinders is well-established across various industries (Sarada et al., 2011). Hence, the research on enhancing HT through the use of inserts in horizontal tubes underscores the significance of ongoing studies, demanding considerable attention to scrutinize their inherent characteristics. Since the late 1990s when hexagonal perforated tube inserts (HPT) were discovered as a means of HT enhancement, there has been a consistent upward trend in investigating the ideal insert types with respect to HT modes (Assari et al., 2023; Gabir and Alkhafaji, 2021). This suggests that researchers are gradually filtering out less effective methods while simultaneously identifying new insert types and advancing potential techniques in pursuit of achieving optimal HT rates.

1813-8535 (Print), 2070-8998 (Online) Received on: December, 2023

To date, the literature has encompassed a wide array of inserts, including twisted tape inserts, wire coil inserts, ribbed inserts, baffles, plates, helical screw inserts, mesh inserts, and conical rings (Kanojiya et al., 2014; Bhattacharyya et al., 2021; Nandakumar et al., 2022). Extensive research spanning several decades has been conducted on these inserts by various scholars, aiming to pinpoint the most effective inserts capable of delivering a significant boost in HT while maintaining a reasonable level of pressure drop (Maradiya et al., 2018; Tu et al., 2015; Vaisi et al., 2023; Kore et al., 2023). Eventually, coil wire inserts and twisted tape inserts began to garner more attention than other insert types (Allam et al., 2021). In the early 20th century, Naphon's study (Naphon, 2006) delved into the impact of coil wire inserts in double-pipe heat exchangers using water as the working medium. The wire had a 1 mm diameter and was fashioned into a coil with a 7.80 mm diameter. This investigation yielded a notable enhancement in HT within the laminar flow regime, with a gradual decline in effectiveness as the Reynolds number (*Re*) increased.

Garcia et al., (2005) conducted an experimental analysis of HT performance using helical wire coil inserts within a round tube spanning from laminar to turbulent flows. Their observations revealed a nine-fold increase in pressure drop and a four-fold increase in HT under turbulent conditions when compared to the results of a plain tube. Notably, the helical coil wire inserts demonstrated superior performance in the transition flow region compared to laminar regimes. Building on this work, Gracia et al., (2012) extended their investigations to assess the thermal performance of corrugated tubes, dimpled tubes, and coiled wire inserts. They found that incorporating coil wire inserts yielded the most benefits when Re ranged between 200 and 2000. Noothong et al., (2006) explored the impact of twisted tape inserts with varying twist ratios in a double pipe HE, utilizing air and water as HT mediums. The maximum average Nusselt numbers (Nuavg) observed were 188% and 159% higher than those of a plain tube when using twist tapes with twist ratios of 5 and 7, respectively. Several other studies aimed at quantifying HT enhancement. Sundar and Sharma (2010) achieved a 33.51% total enhancement in HT using twisted tapes with nanofluids at turbulent flow, while Hejazi et al., (2010) concluded that the incorporation of twisted tape inserts resulted in a 40% overall increment compared to a plain tube.

Furthermore, persistent efforts have been invested in comparing HT enhancement performance of coiled wire inserts and twisted tape inserts. In an experimental study conducted by Wang and Sunden (2002), a comparison was made between HT rates of coiled wire inserts and twisted tape inserts. They found that twisted tape inserts delivered approximately 42% higher heat performance than coiled wire inserts when the pressure drop was not factored in. Conversely, coiled wire inserts exhibited superior thermal efficiency when the pressure drop was taken into account. These promising results from insert-based HT enhancement have spurred further research endeavors, aiming to explore the optimal design of inserts. Additionally, researchers have explored modifications to inserts, with an eye toward achieving improved HT enhancement outcomes while considering factors such as material consumption and pressure drop. Rahimi et al. (2009) delved into the performance of classic, perforated, notched, and jagged twisted tape inserts. Their findings concluded that geometric modifications applied to twisted tape inserts led to greater HT enhancement by introducing higher turbulent intensity near the tube wall surfaces. Results indicated an approximate 31% increase in Nu when employing jagged twisted tapes compared to classic twisted tapes. In a separate investigation by Chang et al. (2007), the performance of HT enhancement was studied by incorporating broken twisted tapes, which resulted in a remarkable increase in thermal performance, reaching up to 4.7 times when compared to smooth twisted tape inserts. One notable modification to inserts is perforation, involving the creation of holes through the metal sheet, a feature that has gained prominence.

Numerous researchers have undertaken comparative studies between perforated inserts and conventional inserts. Eiamsa-ard et al. (2009) achieved a superior HT performance of up to 208% with perforated twisted tapes (PTT) inserts in contrast to regular twisted tapes (TT). Mashoofi et al. (2017) also observed enhanced thermal performance with PTT compared to TT, particularly under turbulent conditions at Re = 16000. Furthermore, Bhuiya et al. (2013) recorded a remarkable 340% increase in Nu and a 59% improvement in the thermal performance factor using PTT inserts with varying porosities, as compared to tubes without inserts. Additionally, Suri et al. (2017) reported a notable 5.92-fold increase in Nu with square perforated twisted tapes while maintaining a reasonable level of friction factor. The research conducted by these scholars collectively indicates that perforation features contribute to reducing overall pressure loss. In a similar vein, Salam (2017) investigated HT enhancement using rectangular fins with solid and circular perforations along the lateral axis. This led to improved thermal performance, as evidenced by an increase in Nu and a reduction in pressure drop when circular perforated fins were employed. Moreover, Lei et al. (2012) achieved a further 34.1% to 46.8% enhancement in HT and an 8.0% to 16.1% reduction in friction factor by employing modified twisted tapes in comparison to smooth twisted tape inserts. This reduction in friction factor was attributed to the hole features of the modified twisted tapes, which contributed to alleviating the significant pressure loss observed with smooth twisted tapes.

More details on the flow in the pipe are also available in the literature (Saha and Paul, 2014a, b; 215a, b; 2017; 2018).

The literature has described numerous types of inserts, and many researchers continue to explore new insert designs and potential modifications. It is evident from the literature that altering plain inserts leads to improved HT rates and thermal enhancement factors. This improvement primarily results from the introduction of small gaps through modification features, which effectively manage pressure drop at a reasonable level, consequently enhancing overall thermal performance compared to plain inserts. This not only enhances performance but also conserves energy and materials. Research on improving HT through the use of perforation feature inserts remains relatively limited. Earlier studies have employed circular or square-shaped perforation patterns, with hexagonal perforation designs receiving little attention. In this study, we have optimized the geometric domain and incorporated various flow control parameters to address this gap in the research.

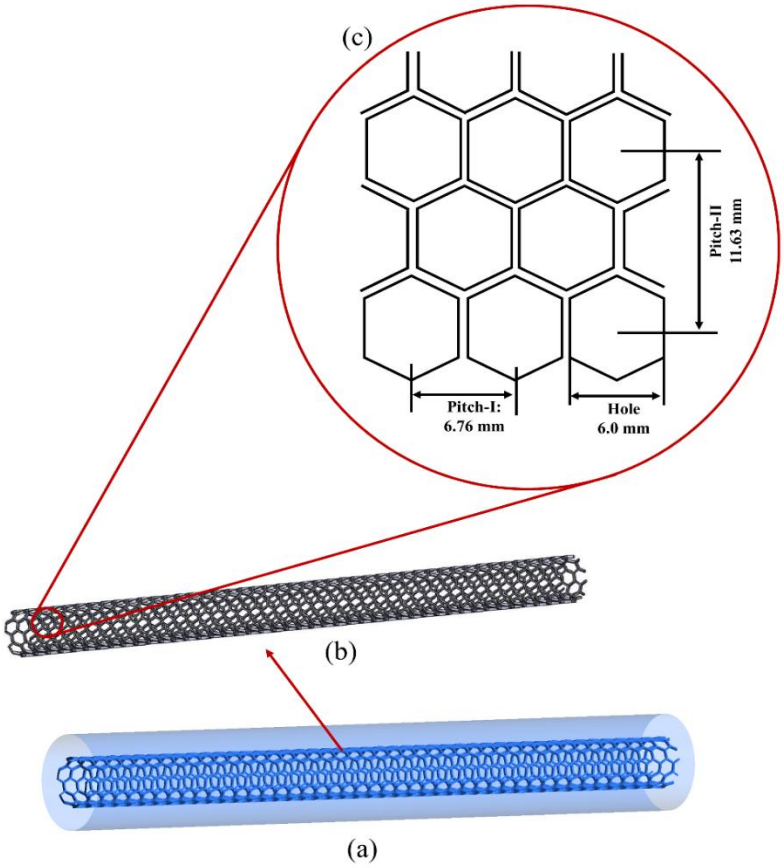

Fig. 1: (a) Schematic design of the physical model, (b) Configuration of hexagonal perforated tube insert, (c) Enlarged view of the tube insert with physical dimensions.

2. Physical Model and Governing Equations

This research aims to develop an efficient heat transfer technology that may be used in a variety of real-world applications, such as heat exchangers, chemical reactors, and air conditioners. ANSYS FLUENT was used to evaluate models of hexagonal perforated tube (HPT) inserts. Examinations have been conducted to assess the convective HT performance utilizing hexagonal perforated tube (HPT) inserts within a horizontal tube of a shell-and-tube HE. The schematic representation of this current research is depicted in Fig. 1, wherein the hexagonal perforated insert is situated within the fluid flow tube. The tube length was set to 3 cm for shell insertion, while a longer plain pipe was used to capture the fully developed profile. The hexagonal pattern perforation serves a specific purpose due to its expansive open area, which promotes enhanced medium mixing and fluid flow within the horizontal tube without encountering significant obstructions. The hexagonal pattern on the tube's surface has been meticulously designed, covering up to 79% of the open area, a strategic approach that minimizes material consumption and, consequently, reduces the weight of HE. The hydraulic diameter of the horizontal tube was standardized at 0.042 meters, and various diameter ratios of HPT have been analyzed in this investigation. The

tube was engineered with a hole diameter of 6.0 mm, a pitch-I distance of 6.76 mm, and a pitch-II distance of 11.63 mm, as depicted in Fig. 1c. The investigation focused especially on the performance gains that were seen at different flow conditions. The paper then attempts to evaluate performance parameters, such as Nusselt number, Heat flux, and performance analysis, empirically for HTP inserts with profile cuts at various flow controlling parameters.

In this study, the Navier-Stokes equations are employed to describe the behaviour of the medium, particularly when dealing with air as the primary fluid, which is assumed to exhibit Newtonian properties. These equations, along with the energy transport equations, make the assumption that the air medium is steady-state, three-dimensional, incompressible, and devoid of chemical reactions. Additionally, various factors such as buoyancy, phase changes, and HT through radiation and conduction are omitted from consideration to maintain simplicity in this study. It is presumed that other thermophysical characteristics of the air medium remain constant. Therefore, the fundamental mathematical equations governing this flow phenomena encompass continuity, momentum, and energy equations are given below (Saha et al., 2010; Xu and Saha, 2014; Al zahrani et al., 2020):

$$\left.\begin{array}{c} \nabla.\left(\rho\vec{v}\right) = 0 \\ \nabla.\left(\rho\vec{v}\vec{v}\right) = -\nabla p + \nabla.\left(\mu\,\nabla\vec{v}\right) \\ \nabla.\left(\rho C_p\vec{v}\,T\right) = \nabla.\left(\kappa\,\nabla T\right) \end{array}\right\} \tag{1}$$

where ρ is the density, κ is the thermal conductivity, μ is the dynamic viscosity, p is the pressure, T is the temperature, $\vec{v}$ is the velocity vector, and C_p is the heat capacity at constant pressure.

In laminar flow considerations, HT approach is distinguished in terms of the dimensionless quantity known as the Nusselt number (*Nu*). Hence, the study mainly is focused on the convective HT by *Nu* which is expressed in Eq. 2. The ratio of convective to conductive heat transfer is estimated by the non-dimensional quantity Nusselt number. It is commonly applied to calculate the efficiency of fluid flow in transmission heat from lower heat energy to higher heat region. The *Nu* for forced convection inside a tube or pipe with HTP inserts can be determined by using Eq. (3) according to the study conducted by Kadbhane and Pangavhane (2024):

$$Nu = \frac{q_{conv}\,D}{(T_w - T_m)\,\kappa}, T_m = \frac{1}{2}(T_{in} + T_{out}) \tag{2}$$

$$Nu = 0.214 \times (Re^{0.8} - 100) \times Pr^{0.4} \tag{3}$$

3. Numerical Method

3.1 Model formulation

The precise numerical approach employed here provides a detailed explanation of the computations involved in utilizing a HPT insert to enhance convection within a horizontal tube under laminar flow conditions. This investigation encompasses an analysis of fluid flow and HT, which leverages meticulously devised simulation techniques based on computational fluid dynamics (CFD). To conduct this analysis, numerical simulations of the governing equations were executed using the commercially available simulation software ANSYS Fluent (version: 19.2), in conjunction with SolidWorks for designing the three-dimensional model. The simulation was configured with a sequential algorithm to attain a stable solution, employing the SIMPLE algorithm as the pressure-velocity coupling method and the QUICK scheme for solving the energy and momentum equations. The inlet boundary and initial conditions were set to a fixed axial velocity, while the outlet condition was maintained at the average static pressure, equivalent to standard atmospheric pressure. All tube walls remained stationary, and a non-slip boundary condition was applied. A constant wall temperature of 380 K was maintained. The laminar flow experiments were carried out at three distinct ranges of Re. Table 1 provides an overview of the parameters controlling the flow and other thermophysical properties within the fluid domain.

Table 1: Initial and boundary conditions applied in this study.

Parameters/Properties	Values
Inlet velocity	0.4, 0.5 and 0.6
Re	1118, 1397 and 1676
ρ	1.205
μ	1.81×10^{-5}
κ	0.027

3.2 Grid refinement tests

The entire computational domain for the cylindrical structure, including HPT insert, was modelled. Commercial software ANSYS Fluent 19.2 was employed to create this domain, using a tetrahedral grid structure. This grid consisted of a varying number of nodes, ranging from 47,360 to 168,279, and was generated using a multi-zone meshing approach, illustrated in Fig. 2. To enhance accuracy, inflation techniques were applied in areas with higher grid concentration, such as near-wall contact regions and insert-fluid contact regions. Additionally, a denser mesh was employed at radial angles to ensure proper resolution of intricate flow patterns.

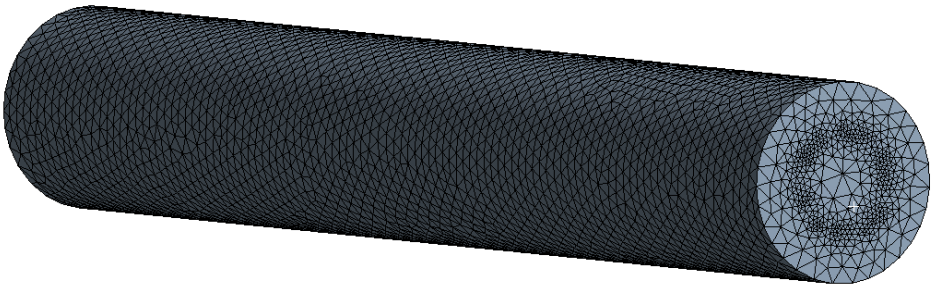

Fig. 2: Computational mesh structure of the domain.

Grid refinement tests were conducted to assess the stability of the mesh generated within the domain and to determine the most suitable mesh configuration for achieving highly accurate numerical solutions. In the context of this study, five distinct grid refinement tests were executed, corresponding to the utilization of five different models illustrated in Fig. 3. One model featured a plain horizontal tube, while the remaining four incorporated HPT inserts with varying *DR*. Notably, the mesh size was inversely related to the number of nodes, with the densest mesh having the smallest grid size. Throughout the grid resolution analysis, outlet velocities were extracted for each grid size.

As illustrated in Fig. *3a*, the computed grid sizes ranged from 8,906 to 266,236 nodes, and the outlet velocities displayed minimal variation between grid sizes 114,456 and 266,236. The consistency of these computational outcomes underscores the fact that the solution's accuracy hinges on the number of cells into which the domain is divided. Consequently, a mesh size of 114,456 nodes was chosen for all simulations involving the plain tube investigation, ensuring efficient computational time utilization without compromising result accuracy. Similarly, for Figs. *3*(*b to e*), representing HPT inserts A to D, the selected grid sizes were 168,279, 47,360, 99,138, and 138,876 nodes. These choices were based on the convergence of results while maintaining an optimal computational cost. These grid configurations were correspondingly employed for post-processing procedures. The velocity profiles for each model reached a stable level, confirming that the models were well-converged at the minimum grid size.

3.3 Model validation

The validation of numerical findings against previous experimental data is a critical step in assessing their alignment with established correlations. The equations (Eq. 2 and Eq. 3) have been used to calculate the Nusselt number for both experimental and numerical studies. An experimental study, conducted under identical parameter conditions as the computational investigation, featured a comprehensive experimental setup depicted in Fig. 4. Moreover, Fig. 5 provides a side-by-side comparison of *Nu* values obtained from both experiments and numerical simulations for plain tubes and tubes equipped with the HPT-A insert across various *Re* conditions. Remarkably, the computed *Nu* values for HPT-A from the computational model consistently exceeded the corresponding experimental *Nu* values. Conversely, *Nu* values for plain tubes were consistently underestimated across all *Re* ranges. The increase in *Re* is attributed to the growing prominence of fluid viscous forces, leading to reduced shear between the fluid and the tube wall, responsible for increased momentum (Holman, 2010). However, the disparities observed in *Nu* between the numerical and experimental results may stem from variations in the experimental conditions, yielding different *Nu* quantities. Inevitable factors include the inclusion of conduction and radiation HT conditions in the experimental setup and fluctuations in the current and voltage supplied from the laboratory, potentially affecting the air flow velocity from the blower during the experimental studies. Calibrating uncertainties in the devices used in the experiment could also contribute to variations in the final investigation results. Furthermore, in the experimental configuration, convection heat fluxes were assumed to be constant for all cases, diverging from the numerical investigation where individual heat fluxes were efficiently computed using software. These collective factors contribute to the distinctions between the experimental and numerical results.

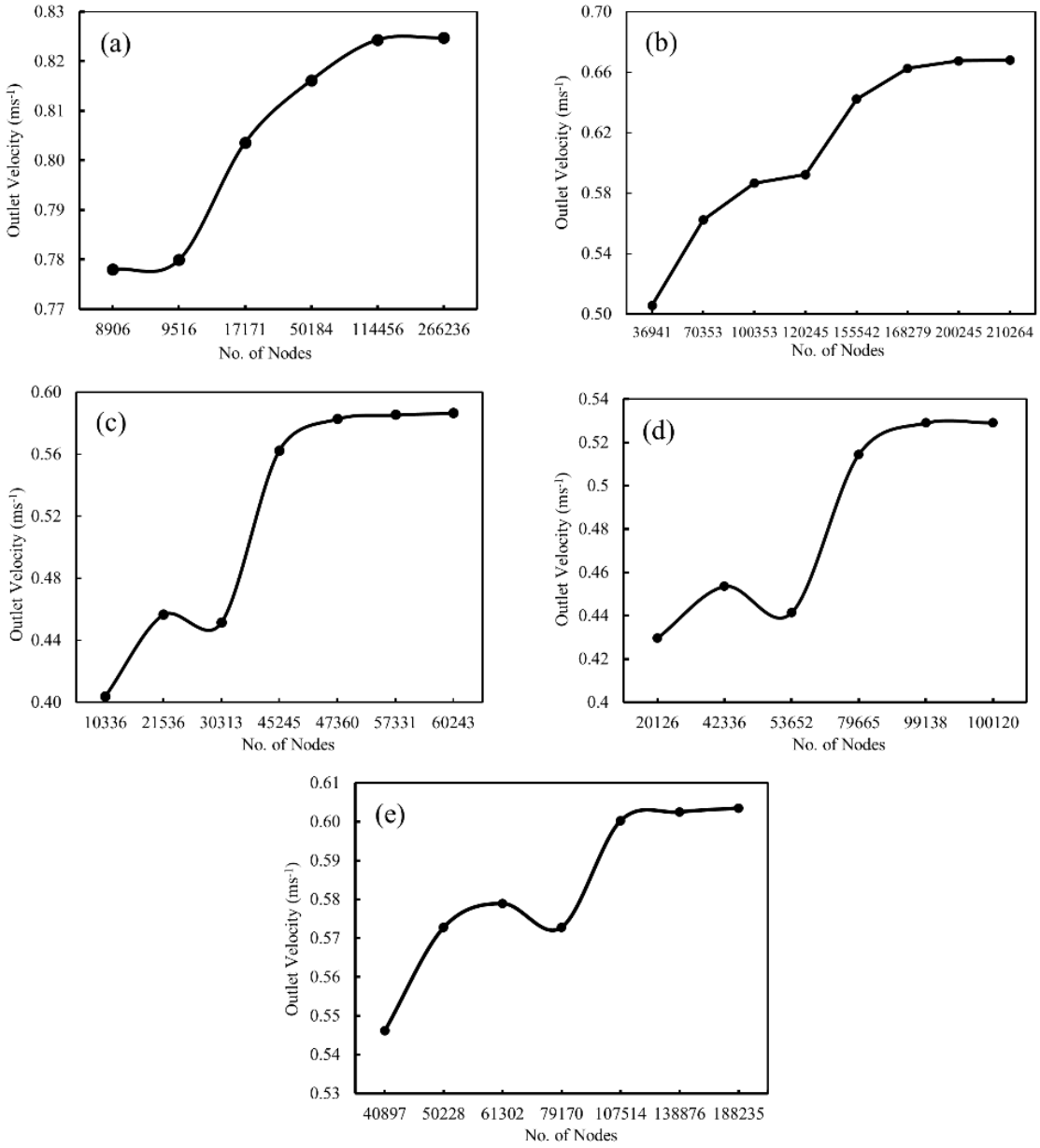

Fig. 3: Grid refinement test at various grid sizes. (a) Velocity distribution for plain tube, (b) Velocity distribution for HPT - A insert, (c) Velocity distribution for HPT - B insert, (d) Velocity distribution for HPT - C insert, (e) Velocity distribution for HPT - D insert.

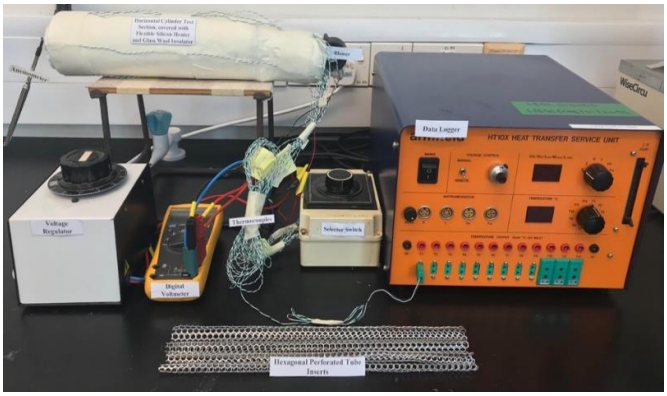

Fig. 4: Image of the experimental configuration.

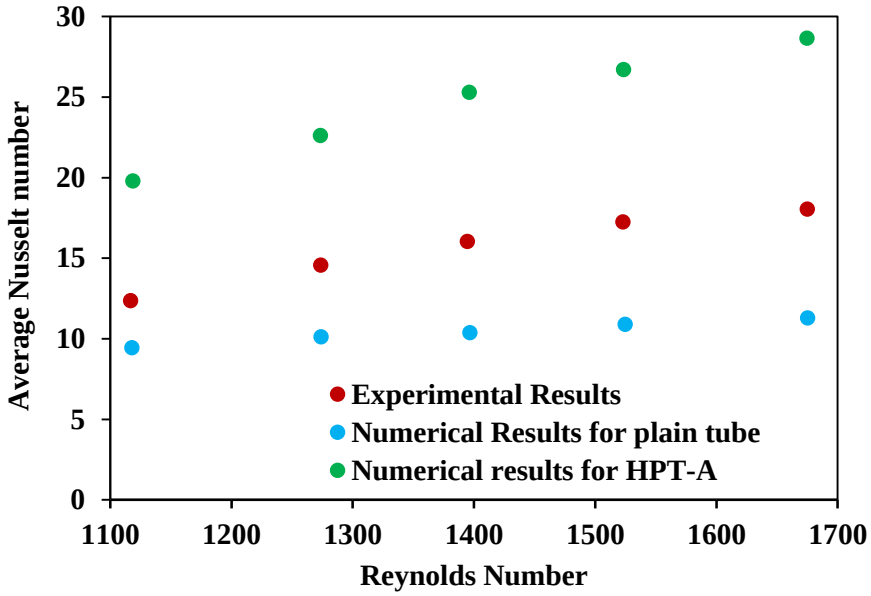

Fig. 5: Comparison between experimental results and numerical results for the model validation in the case of plain tube and HPT - A inserts.

The proposed model was comprehensively validated with another experimental study by Naik et al. (2013). We built a computational domain based on their protocol and used similar flow conditions. We monitored the average Nusselt number relative to Reynolds numbers, optimizing flow conditions and geometry through trial and error. Figure 6 shows the mean Nu as a function of Reynolds number, revealing a consistent upward trend with minimal fluctuation that aligns with experimental findings.

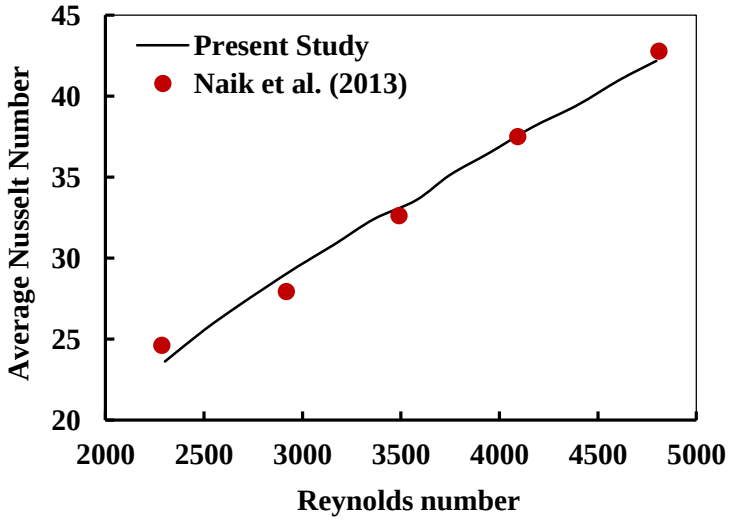

Fig. 6: Comparison of averaged Nusselt number as the function Reynolds number from present study with numerical findings from Naik et al. (2013) study.

4. Results and Discussion

In this section, we explore the enhancement of convective HT effects. We also analyze and discuss various aspects, including temperature and velocity contours, convective heat flux, as well as *Nu* within the numerical domain.

4.1 Temperature contours

Temperature profiles, particularly at the outlet and along the tube, were visualized through the creation of temperature contours for both the plain tube and tubes equipped with HPT inserts, as depicted in Fig. 7 (a and b).

In Fig. 7a, temperature contours extracted from the plain tube at different *Re* = 1676, 1397, and 1118 at the outlet are presented. The maximum temperature (T_{max}, 377.6 K) on the plain tube was observed at the outer wall, while the minimum temperature (T_{min}, 300 K) was recorded in the central region of the tube. Furthermore, in Fig. 7b, the outlet temperature contours of tubes fitted with HPT inserts at different DR are illustrated. The development of these contours followed the same heating and *Re* conditions as those of the plain tube. Consequently, upon comparing the temperature contours of the plain tube as shown in Fig. 7a and those of the tube equipped with HPT inserts as shown in Fig. 7b, a notable observation is the temperature increase in tubes with HPT inserts. The average temperature extracted from the tubes enhanced with HPT inserts was found to be up to 4.5% higher than in the plain tube. This temperature increment resulting from the insertion of HPT inserts is attributed to the heightened disturbance within the boundary layer due to increased fluid mixing.

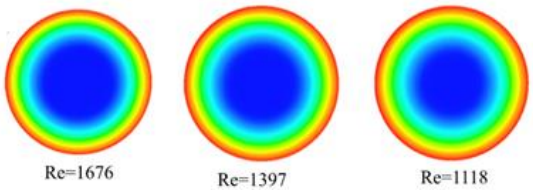

Fig. 7a: Temperature contour plots for different *Re* at outlet of plain tube

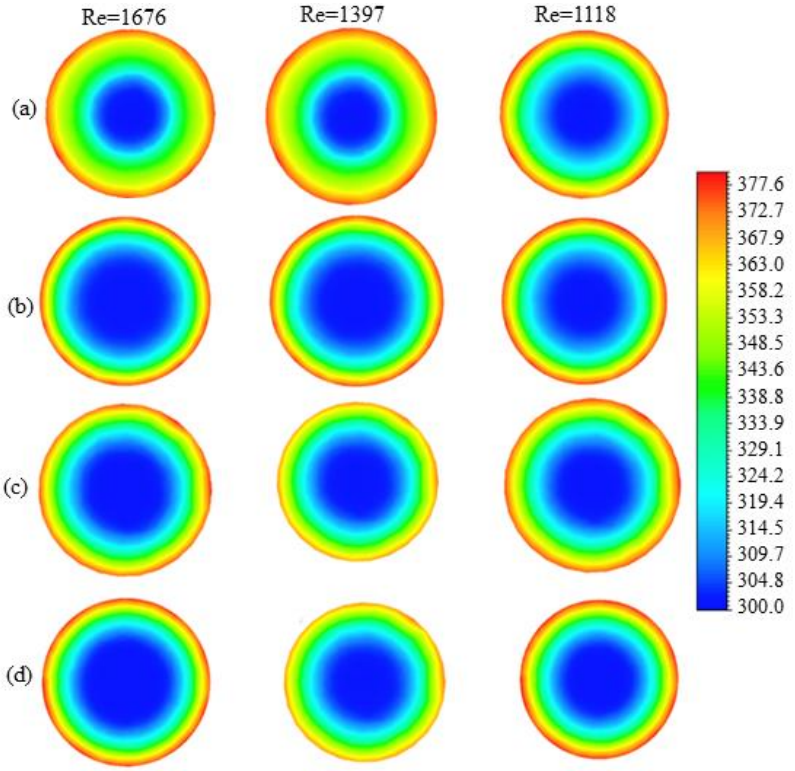

Fig. 7b: Temperature contour plots for different *Re* at outlet of plain tube employed with (a) HPT - A, (b) HPT - B, (c) HPT – C, (d) HPT – D.

4.2 Velocity contours

To gain insights into the fluid dynamics influenced by HPT inserts, velocity contours at the tube outlet were generated for each scenario, as depicted in Fig. 8. Figure 8a illustrates the outlet velocity contours when a plain tube is employed at various *Re*. In all cases with the plain tube, a consistent pattern emerges, with higher velocities concentrated at the tube's center, gradually diminishing near the tube's wall. This pattern suggests fully developed and parabolic flow. In contrast, when comparing the velocity contours obtained with plain tube to those utilizing HPT inserts, a noticeable contrast becomes apparent in Figs. 8 (b-e), showing the outlet velocity contours for tubes equipped with HPT inserts A, B, C, and D, respectively.

The incorporation of HPT inserts brings about notable changes in flow patterns within the tube when contrasted with the plain tube. Examining Figs. 8 (b-e), it becomes evident that the application of HPT inserts has a substantial impact on velocity profiles within the tube. In the depicted figures, the velocity in proximity to the tube wall rises owing to the amplified mixing and swirling effects generated by the HPT inserts. This results in velocity magnitudes of approximately 15.19%, 3.15%, and 6.67% higher for HPT-A, HPT-B, HPT-C, and HPT-D, respectively, at *Re* = 1676. Interestingly, the peak outlet velocity for the tube with HPT-B is approximately 4.88% lower compared to the plain tube. This discrepancy underscores how different HPT insert designs can lead to distinct disturbance effects. Figs. 8 (b-e) show that higher DR of the HPT inserts generate higher velocities within the inserts themselves, while lower DR of HPT inserts lead to higher velocities outside the inserts, between the tube's walls. Consequently, this creates variations in velocity magnitude along the tube, reflecting the disturbance effects brought about by the HPT inserts.

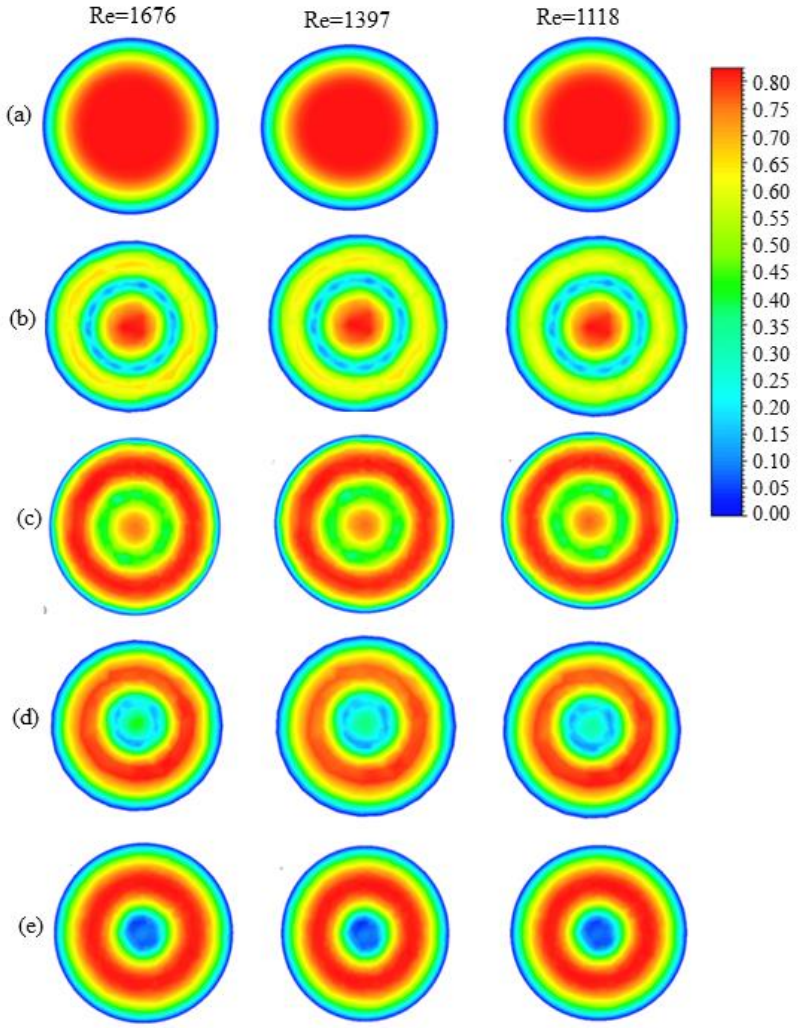

Fig. 8: Velocity contour plots for different *Re* at outlet of the geometry along the cross-section of the cylinder: (a) plain cylinder, (b) HPT-A, (c) HPT-B, (d) HPT-C and (e) HPT-D.

4.3 Heat transfer and heat flux analysis

Figure 9 illustrates the average surface convective heat fluxes. Notably, the heat flux calculated for tubes equipped with HPT inserts significantly surpassed those achieved in plain tubes. Specifically, for *Re* = 1676, the convective heat flux for tubes featuring HPT-A, HPT-B, HPT-C, and HPT-D was 54.5%, 23.2%, 23.6%, and 10.6%, respectively. Similarly, at *Re* = 1397, these values increased by 53.1%, 22.6%, 22.6%, and 10.1% for HPT-A, HPT-B, HPT-C, and HPT-D, respectively. Finally, at *Re* = 1118, we observed respective increments of 56.9%, 21.3%, 21.4%, and 9.7% for HPT-A, HPT-B, HPT-C, and HPT-D. Notably, HPT-A inserts consistently outperformed the other HPT inserts in generating higher convective heat flux.

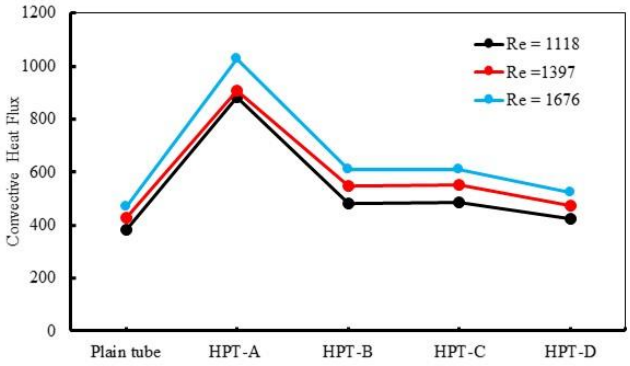

Fig. 9: Convective Heat Flux computed for each of the cylinder with and without HPT inserts.

In this study, we have extracted the local *Nu* values along the dimensionless distance of the tube and presented them in Fig. 10. Figure 10 displays the graphs illustrating the local *Nu* profiles for tubes equipped with HPT-A, HPT-B, HPT-C, and HPT-D at *Re* of 1118, 1397, and 1676. The *Nu* values in these graphs were computed along the dimensionless distance from the tube inlet to the outlet. Observations from the plot panels reveal a consistent trend where the local *Nu* curve gradually decreases from the inlet and stabilizes near the outlet. This behaviour signifies the impact of *Re* on *Nu* for these geometrically modified perforated tube inserts. Given that the distribution of the local *Nu* along the tube predominantly reflects the temperature gradient along its length, the stable curves near the tube's outlet suggest minimal or no variations in temperature, thus indicating the stability of the convective *Nu* in this region.

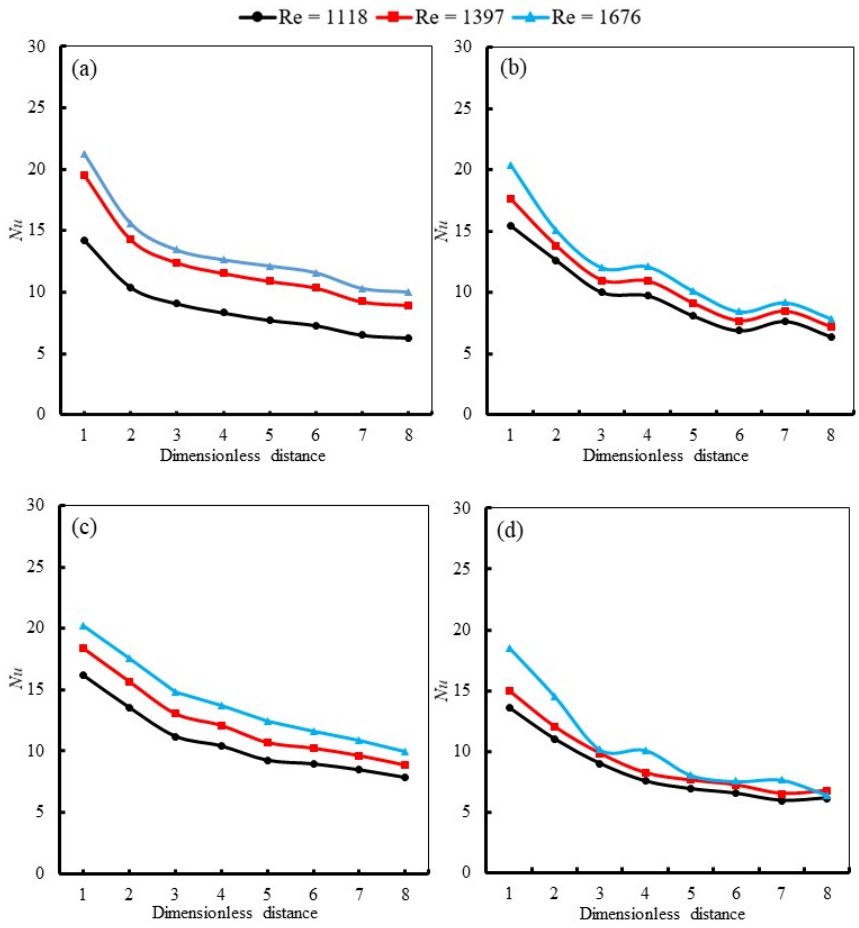

Fig. 10: Local *Nu* along the dimensionless distance of tube induced with (a) HPT-A, (b) HPT-B, (c) HPT-C and (d) HPT-D.

Table 2 displays the percentage improvements in convective *Nu* achieved by HPT-A, HPT-B, HPT-C, and HPT-D in comparison to a plain tube. It is evident that the inclusion of HPT inserts leads to significantly higher convective *Nu* compared to a plain tube. According to the findings of Gou *et al.* (2011), this increase in *Nu*, resulting from the use of inserts, is attributed to a reduction in the cross-sectional area of the flow and an increase in the velocity of the induced tubes, as illustrated in Fig. 8, which enhances swirl flow within the tube. These factors collectively contribute to an increase in HT coefficient of the induced tube. Furthermore, the incorporation of perforated features in the inserts promotes additional swirl flows, further augmenting the velocity magnitude. It is noteworthy that the overall enhancement of *Nu* achieved by HPT-A, HPT-B, HPT-C, and HPT-D at *Re* = 1118 is 52.4%, 20.6%, 13.7%, and 8.7%, respectively. At *Re* = 1397, the *Nu* enhancements are 58.8%, 21.0%, 15.2%, and 8.8% for HPT-A, HPT-B, HPT-C, and HPT-D, respectively. Additionally, at *Re* = 1676, the enhancements in *Nu* are 60.4%, 21.7%, 16.6%, and 8.9% for HPT-A, HPT-B, HPT-C, and HPT-D, respectively. These results clearly indicate that higher *Re* lead to greater improvements in convective *Nu*. Furthermore, a noteworthy insight gleaned from this current study is the influence of DR of HPT inserts on the distribution and magnitude of swirl flows generated within the tube, consequently leading to varying degrees of Nu enhancement. In the context of this study, as evidenced in Table 2, it is evident that a larger DR of the HPT inserts resulted in a greater enhancement of *Nu* (specifically, HPT-A yielded the highest *Nu* enhancement).

Table 2: Percentage of *Nu* enhancement by various HPT inserts.

	Reynolds number (*Re*)		
Models	1118	1397	1676
HPT-A	52.37%	58.76%	60.40%
HPT-B	20.60%	21.02%	21.68%
HPT-C	13.67%	15.16%	16.63%
HPT-D	8.72%	8.81%	8.94%

5. Conclusions

Numerical analysis was conducted to examine the augmentation of *Nu* within a horizontal tube through the utilization of HPT inserts under laminar flow conditions, covering a range of *Re* from 1118 to 1676. The key findings from this study are summarized as follows:

- HPT-A achieved a remarkable convective *Nu* enhancement of up to 60.4% at *Re* = 1676.
- An increase in *Re* leads to a corresponding increase in convective *Nu*, attributed to improved fluid mixing and swirling within the tube.
- DR of the HPT inserts directly impacts flow disturbance and swirl, resulting in varying levels of *Nu* enhancement.

The study presented qualitative results by depicting temperature and velocity contours for both plain tubes and tubes with HPT inserts. Furthermore, the local and average *Nu* distribution was analyzed across different *Re* and *DR* values for HPTs. Additionally, a comparative analysis was conducted to assess the convective *Nu* enhancement between tubes with and without inserts. The insights gained from this investigation hold significant potential for the design of more efficient industrial HT equipment. Thus, this research makes a valuable contribution to the field of enhancing convective heat transfer through the use of passive HPT insert techniques.

References

Allam, M., Tawfik, M., Bekheit, M. and El-Negiry, E. (2021): Heat transfer enhancement in parabolic trough receivers using inserts: A review, Sustainable Energy Technologies and Assessments, Vol. 48, Article No. 101671. https://doi.org/10.1016/j.seta.2021.101671

Ali, M. R., Al-Khaled, K., Hussain, M., Labidi, T., Khan, S. U., Kolsi, L. and Sadat, R. (2023): Effect of design parameters on passive control of heat transfer enhancement phenomenon in heat exchangers–A brief review, Case Studies in Thermal Engineering, Vol. 43, Article No. 102674. https://doi.org/10.1016/j.csite.2022.102674

Al zahrani, S., Islam, M. S., Xu, F. and Saha, S. C. (2020): Thermal performance investigation in a novel corrugated plate heat exchanger, International Journal of Heat and Mass Transfer, Vol. 148, Article No. 119095. https://doi.org/10.1016/j.ijheatmasstransfer.2019.119095

Assari, M., Banihashemi, S., Setareh, M. and Nargesi Motlagh, A. M. (2023): Numerical study of thermal characteristics and pressure drop in a pipe equipped with innovative perforated and hollow spherical inserts, Journal of Thermal Analysis and Calorimetry, Vol. 148, No. 20, pp. 11325–11348.

https://doi.org/10.1007/s10973-023-12422-8

Bhattacharyya, S., Pathak, M., Sharifpur, M., Chamoli, S. and Ewim, D. R. E. (2021): Heat transfer and exergy analysis of solar air heater tube with helical corrugation and perforated circular disc inserts, Journal of Thermal Analysis and Calorimetry, Vol. 145, No. 3, pp. 1019–1034. https://doi.org/10.1007/s10973-020-10215-x

Bhattacharyya, S., Vishwakarma, D. K., Srinivasan, A., Soni, M. K., Goel, V., Sharifpur, M., Ahmadi, M. H., Issakhov, A. and Meyer, J. (2022): Thermal performance enhancement in heat exchangers using active and passive techniques: a detailed review, Journal of Thermal Analysis and Calorimetry, Vol. 147, No. 17, pp. 9229–9281. https://doi.org/10.1007/s10973-021-11168-5

Bhuiya, M. M. K., Chowdhury, M. S. U., Saha, M. and Islam, M. T. (2013): Heat transfer and friction factor characteristics in turbulent flow through a tube fitted with perforated twisted tape inserts, International Communications in Heat and Mass Transfer, Vol. 46, pp. 49–57.

https://doi.org/10.1016/j.icheatmasstransfer.2013.05.012

Chang, S. W., Yang, T. L. and Liou, J. S. (2007): Heat transfer and pressure drop in tube with broken twisted tape insert, Experimental Thermal and Fluid Science, Vol. 32, No. 2, pp. 489–501.

https://doi.org/10.1016/j.expthermflusci.2007.06.002

Dhumal, A. H., Kerkal, G. M. and Pawale, K. T. (2017): Heat transfer enhancement for tube in tube heat exchanger using twisted tape inserts, International Journal of Advanced Engineering Research and Science, Vol. 4, No. 5, pp. 89–92. https://doi.org/10.22161/ijaers.4.5.15

Eiamsa-ard, S., Thianpong, C., Eiamsa-ard, P. and Promvonge, P. (2009): Convective heat transfer in a circular tube with short-length twisted tape insert, International Communications in Heat and Mass Transfer, Vol. 36, No. 4, pp. 365–371. https://doi.org/10.1016/j.icheatmasstransfer.2009.01.006

Gabir, M. M. and Alkhafaji, D. (2021): Comprehensive review on double pipe heat exchanger techniques, Journal of Physics: Conference Series, Vol. 1973, No. 1, Article No. 12013. https://doi.org/10.1088/1742-6596/1973/1/012013

García, A., Vicente, P. G. and Viedma, A. (2005): Experimental study of heat transfer enhancement with wire coil inserts in laminar-transition-turbulent regimes at different Prandtl numbers, International Journal of Heat and Mass Transfer, Vol. 48, No. 21, pp. 4640–4651. https://doi.org/10.1016/j.ijheatmasstransfer.2005.04.024

García, A., Solano, J. P., Vicente, P. G. and Viedma, A. (2012): The influence of artificial roughness shape on heat transfer enhancement: Corrugated tubes, dimpled tubes and wire coils, Applied Thermal Engineering, Vol. 35, No. 1, pp. 196–201. https://doi.org/10.1016/j.applthermaleng.2011.10.030

Guo, J., Fan, A., Zhang, X. and Liu, W. (2011): A numerical study on heat transfer and friction factor characteristics of laminar flow in a circular tube fitted with center-cleared twisted tape, International Journal of Thermal Sciences, Vol. 50, No. 7, pp. 1263–1270. https://doi.org/10.1016/j.ijthermalsci.2011.02.010

Hejazi, V., Akhavan-Behabadi, M. A. and Afshari, A. (2010): Experimental investigation of twisted tape inserts performance on condensation heat transfer enhancement and pressure drop, International Communications in Heat and Mass Transfer, Vol. 37, No. 9, pp. 1376–1387. https://doi.org/10.1016/j.icheatmasstransfer.2010.07.021

HEMT: Heat Exchanger Market by Technology (Shell and Tube, Plate, Air Cooled, Others), By Application (Oil and Gas, Chemical, Power Generation and Metallurgy, Marine, Mechanical Industry, Central Heating and Refrigeration, Food Processing, Others), Industry Analysis Report, Regional Outlook, Application Potential, Competitive Market Share and Forecast, 2019 - 2025. Report ID: GMI3169. Link: https://www.gminsights.com/industry-analysis/heat-exchanger-market Accessed on 30 November 2023.

Holman, J. P. (2010): Heat Transfer. 10th Edition, New York: McGraw-Hill. ISBN: 0073529362, 9780073529363

Kadbhane, S. V., and Pangavhane, D. R. (2024): Performance prediction and evaluation of heat pipe with hexagonal perforated twisted tape inserts. Heat and Mass Transfer, Vol. 60, No. 6, pp. 987-1008. https://doi.org/10.1007/s00231-024-03469-w

Kanojiya, N. C., Kriplani, V. M. and Walke, P. V. (2014): Heat transfer enhancement in heat exchangers with inserts: A review, International Journal of Engineering Research and Technology (IJERT), Vol. 3, No. 10, pp. 494-500.

Kore, S. S., Chaudhary, M. K., Patil, A. S. and Kolate, V. D. (2023): Computational study and enhancement of heat transfer rate by using inserts introduced in a heat exchanger, Journal of Advanced Research in Fluid Mechanics and Thermal Sciences, Vol. 103, No. 1, pp. 16–29. https://doi.org/10.37934/arfmts.103.1.1629

Kundan, L. and Darshan, M. B. (2022): Performance investigation of a concentric double tube heat exchanger using twisted tape inserts and nanofluid, Particulate Science and Technology, Vol. 40, No. 3, pp. 307–324. https://doi.org/10.1080/02726351.2021.1946729

Lei, Y. G., Zhao, C. H. and Song, C. F. (2012): Enhancement of turbulent flow heat transfer in a tube with modified twisted tapes, Chemical Engineering and Technology, Vol. 35, No. 12, pp. 2133–2139. https://doi.org/10.1002/ceat.201200218

Maradiya, C., Vadher, J. and Agarwal, R. (2018): The heat transfer enhancement techniques and their thermal performance factor, Beni-Suef University Journal of Basic and Applied Sciences, Vol. 7, No. 1, pp. 1–21. https://doi.org/10.1016/j.bjbas.2017.10.001

Mashoofi, N., Pourahmad, S. and Pesteei, S. M. (2017): Study the effect of axially perforated twisted tapes on the thermal performance enhancement factor of a double tube heat exchanger, Case Studies in Thermal Engineering, Vol. 10C, pp. 161–168. https://doi.org/10.1016/j.csite.2017.06.001

Mohammed, H. A., Hasan, H. A. and Wahid, M. A. (2013): Heat transfer enhancement of nanofluids in a double pipe heat exchanger with louvered strip inserts, International Communications in Heat and Mass Transfer, Vol. 40, No. 1, pp. 36–46. https://doi.org/10.1016/j.icheatmasstransfer.2012.10.023

Naik, M.T., Janardana, G.R., L. and Sundar, L.S. (2013): Experimental investigation of heat transfer and friction factor with water–propylene glycol based CuO nanofluid in a tube with twisted tape inserts. International Communications in Heat and Mass Transfer, Vol. 46, pp. 113-21. https://doi.org/10.1016/j.icheatmasstransfer.2013.05.007

Nandakumar, P., Loganathan, D., Natarajan, D. P. and Manikandan, P. (2022): Shell and tube heat exchangers in the food industry. In Thermal processing of food products by steam and hot water: Unit operations and processing equipment in the food industry (pp. 153–179). https://doi.org/10.1016/B978-0-12-818616-9.00004-3

Naphon, P. (2006): Effect of coil-wire insert on heat transfer enhancement and pressure drop of the horizontal concentric tubes, International Communications in Heat and Mass Transfer, Vol. 33, No. 6, pp. 753–763. https://doi.org/10.1016/j.icheatmasstransfer.2006.01.020

Noothong, W., Eiamsa-ard, S. and Promvonge, P. (2006): Effect of twisted-tape inserts on heat transfer in a tube, Second Joint International Conference on Sustainable Energy and Environment (SEE 2006), pp. 1-5.

Paneliya, S., Khanna, S., Patel, U., Prajapati, P. and Mukhopadhyay, I. (2020): Systematic investigation on fluid flow and heat transfer characteristic of a tube equipped with variable pitch twisted tape, International Journal of Thermofluids, Vol. 1-2, Article No. 100005. https://doi.org/10.1016/j.ijft.2019.100005

Rahimi, M., Shabanian, S. R. and Alsairafi, A. A. (2009): Experimental and CFD studies on heat transfer and friction factor characteristics of a tube equipped with modified twisted tape inserts, Chemical Engineering and Processing, Vol. 48, No. 3, pp. 762–770. https://doi.org/10.1016/j.cep.2008.09.007

Saha, G. and Paul, M. C. (2014a). Numerical analysis of the heat transfer behaviour of water based Al_2O_3 and TiO_2 nanofluids in a circular pipe under the turbulent flow condition, International Communications in Heat and Mass Transfer, Vol. 56, pp. 96–108. https://doi.org/10.1016/j.icheatmasstransfer.2014.06.008

Saha, G. and Paul, M. C. (2014b): Discrete phase approach for nanofluids flow in pipe, International Journal of Material Science and Engineering-IJMSE, Vol. 2, No. 1, pp. 39-43.

Saha, G. and Paul, M. C. (2015a): Analysis of heat transfer and entropy generation of TiO_2-water nanofluid flow in a pipe under transition, Procedia Engineering, Vol. 105, pp. 381–387.

https://doi.org/10.1016/j.proeng.2015.05.023

Saha, G. and Paul, M. C. (2015b). Heat transfer and entropy generation of turbulent forced convection flow of nanofluids in a heated pipe, International Communications in Heat and Mass Transfer, Vol. 61, pp. 26–36. https://doi.org/10.1016/j.icheatmasstransfer.2014.11.007

Saha, G. and Paul, M. C. (2017): Transition of nanofluids flow in an inclined heated pipe, International Communications in Heat and Mass Transfer, Vol. 82, pp. 49–62. https://doi.org/10.1016/j.icheatmasstransfer.2017.02.017

Saha, G. and Paul, M. C. (2018): Investigation of the characteristics of nanofluids flow and heat transfer in a pipe using a single phase model, International Communications in Heat and Mass Transfer, Vol. 93, pp. 48–59. https://doi.org/10.1016/j.icheatmasstransfer.2018.03.001

Saha, S. C., Patterson, J. C. and Lei, C. (2010): Natural convection boundary-layer adjacent to an inclined flat plate subject to sudden and ramp heating, International Journal of Thermal Sciences, Vol. 49, No. 9, pp. 1600-1612. https://doi.org/10.1016/j.ijthermalsci.2010.03.017

Salam, N. (2017): Heat transfer enhancement through perforated fin, IOSR Journal of Mechanical and Civil Engineering, Vol. 17, No. 10, pp. 72–78. https://doi.org/10.9790/1684-17010047278

Sarada, S. N., Raju, A. S. R., Radha, K. K. and Sunder, L. S. (2011): Enhancement of heat transfer using varying width twisted tape inserts, International Journal of Engineering, Science and Technology, Vol. 2, No. 6. https://doi.org/10.4314/ijest.v2i6.63702

Sundar, L. S. and Sharma, K. V. (2010): Turbulent heat transfer and friction factor of Al_2O_3 nanofluid in circular tube with twisted tape inserts, International Journal of Heat and Mass Transfer, Vol. 53, No. 7-8, pp. 1409–1416. https://doi.org/10.1016/j.ijheatmasstransfer.2009.12.016

Suri, A. R. S., Kumar, A. and Maithani, R. (2017): Heat transfer enhancement of heat exchanger tube with multiple square perforated twisted tape inserts: Experimental investigation and correlation development, Chemical Engineering and Processing, Vol. 116, pp. 76–96. https://doi.org/10.1016/j.cep.2017.02.014

Tu, W., Tang, Y., Hu, J., Wang, Q. and Lu, L. (2015): Heat transfer and friction characteristics of laminar flow through a circular tube with small pipe inserts, International Journal of Thermal Sciences, Vol. 96, pp. 94–101. https://doi.org/10.1016/j.ijthermalsci.2015.04.013

Vaisi, A., Moosavi, R., Javaherdeh, K., Sheikh Zahed, M. V. and Soltani, M. M. (2023): Experimental examination of condensation heat transfer enhancement with different perforated tube inserts, Experimental Heat Transfer, Vol. 36, No. 2, pp. 183–209. https://doi.org/10.1080/08916152.2021.1991510

Wang, L. and Sundén, B. (2002): Performance comparison of some tube inserts, International Communications in Heat and Mass Transfer, Vol. 29, No. 1, pp. 45–56. https://doi.org/10.1016/S0735-1933(01)00323-2

Xu, F. and Saha, S. C. (2014): Transition to an unsteady flow induced by a fin on the sidewall of a differentially heated air-filled square cavity and heat transfer, International Journal of Heat and Mass Transfer, Vol. 71, pp. 236–244. https://doi.org/10.1016/j.ijheatmasstransfer.2013.12.019